TEXAS TECH UNIVERSITY
Libraries™

MODELING PHOSPHORUS ADSORPTION ONTO POLYALUMINIUM CHLORIDE WATER TREATMENT RESIDUALS

Modeling phosphorus adsorption onto polyaluminium chloride water treatment residuals

Runbin Duan and Clifford B. Fedler

ABSTRACT

Beneficial reuse and appropriate disposal of water treatment residuals (WTRs) are of great concern for sustainable drinking water treatment. Using WTRs to remove phosphorus (P) is widely regarded as a feasible approach. However, the information is still limited on air-dried WTRs containing polyaluminium chloride (PAC) and anionic polyacrylamide (APAM) used to adsorb P. The objectives of this study were to construct artificial neural network (ANN) models for P adsorption onto WTRs from distilled de-ionized (DDI) water solution and stormwater, to investigate the performance of ANN in predicting phosphorous adsorption, and to model isotherm adsorption, kinetics, and thermodynamics by using the index of model performance. Batch experiments were performed with different WTRs dosage, pH, initial P concentration, temperature, and time. ANN models accurately predicted the P concentration at equilibrium. Non-linearized Langmuir model fitted the isotherm data best. Pseudo second-order kinetic model provided a better fit to experimental data. The adsorption process may be at least simultaneously controlled by surface adsorption and intraparticle diffusion. The P adsorption is a homogenous monolayer adsorption that is spontaneous, endothermic, and entropy production process. WTRs were found to be favorable and effective in removing P, but the P removals had significant differences in both solutions.

Key words | anionic polyacrylamide, artificial neural network, index of model performance, polyaluminium chloride, WTRs

Runbin Duan (corresponding author)
Department of Environmental Engineering, College of Environmental Science and Engineering,
Taiyuan University of Technology,
Taiyuan, 030024,
China
E-mail: *duanttu@gmail.com*

Clifford B. Fedler
Department of Civil, Environmental, and Construction Engineering,
Texas Tech University,
Lubbock, Texas, 79409,
USA

HIGHLIGHTS

- ANN models can accurately predict the P concentration at equilibrium.
- Non-linearized Langmuir model fitted the isotherms data better than others.
- Pseudo second-order kinetic model predicted experimental data better than others.
- WTRs containing PAC and APAM were effective in removing P from stormwater.
- P removals had significant differences in DDI water solution and stormwater.

INTRODUCTION

Water treatment residuals (WTRs), also named waterworks sludge (Al-Tahmazi & Babatunde 2016) or water treatment plants sludges (Krishna *et al.* 2016), are waste by-products produced during drinking water treatment from most of the municipalities in the world. The reuse and appropriate disposal of WTRs are of great concern for sustainable drinking water treatment. With the population increasing, coupled with the increase in expected quality of life and rapid urbanizing, the global demand of drinking water has been growing exponentially (Dassanayake *et al.* 2015). As a result, the amount of WTRs produced from the expansions of the global drinking water treatment facilities is increasing rapidly. For example, in 2014, the amount of dewatered WTRs produced was 22,000,000 metric tons (containing

doi: 10.2166/ws.2020.322

about 70% water) for China alone. The major WTRs disposal method is the landfill. Unfortunately, landfilling with WTRs often limits the sustainability of drinking water treatment since it requires huge land costs and long-distance transportation; meanwhile, the disposal method is questioned in terms of environmental sustainability.

Environmental professionals have been exploring sustainable approaches to reuse or recycle WTRs for a few decades because they are low cost and readily available in large quantities. Relative research includes aluminum recovery, agricultural land application by using WTRs as a soil ameliorant or a potting media (Ippolito *et al.* 2011), and environmental applications by using WTRs as a coagulant, co-conditioner, or adsorbent for the removal of heavy metals, phosphorous (P), and other pollutants in wastewater treatment. Almost all countries have stringent regulations on the selection, protection and management of surface water sources and the subsequent treatment for drinking water production, and it is impossible for WTRs to contain substantial harmful or toxic substances (Babatunde *et al.* 2009). Many studies have indicated that WTRs can provide P adsorption capacity due to its relatively large specific area and strong affinity for P (Babatunde *et al.* 2009). Therefore, WTRs are widely regarded as a potential environment-friendly P adsorbent (Babatunde *et al.* 2009). However, although researchers have been seeking cost-effective alternatives to partially replace traditional soil-based media in stormwater bioretention systems to control and remove some pollutants, information on the application of WTRs used as the media for P removal from stormwater runoff remains insufficient.

Previous studies indicate that P sorption by WTRs is considerably different, caused by the differences in the formation of WTRs, particle size, and agitation speed adopted during adsorption experiments (Ippolito *et al.* 2011; Al-Tahmazi & Babatunde 2016). Based on the water sources, WTRs can be grouped into surface water WTRs and groundwater WTRs (Krishna *et al.* 2016). Also, WTRs can be primarily classified as aluminium-based WTRs and ferric-based WTRs, considering the coagulants added during the water production process. For aluminium-based WTRs, previous associated studies mostly concentrated on the WTRs with aluminium sulfate or aluminium chloride as the coagulant, yet there are few reports on WTRs with polyaluminium chloride (PAC). Additionally, previous studies did not clarify the dewatering agent used in the dewatering process of the WTRs. Recently, more water treatment plants have used PAC as the coagulant and anionic polyacrylamide (APAM) as the dewatering agent throughout the world, and especially in China. Therefore, it is necessary to investigate P adsorption onto the type of WTRs mentioned.

Artificial neural network (ANN) is a tool used for simulating and predicting the outcomes of a multi-variable environmental system. ANN have been successfully applied to many fields of environmental science and engineering to analyze various relationships in complicated environmental systems (Abba & Elkiran 2017). However, information on using ANN to model phosphorous adsorption onto WTRs is limited. Comparison of models describing isotherm adsorption and adsorption kinetics is mostly conducted by comparing the R^2 of multiple linearized models. In order to more fully understand the performance of these models, an index of model performance should be utilized.

The objectives of this study were to construct ANN models for P adsorption from distilled de-ionized (DDI) water solution and stormwater onto WTRs produced from the water treatment process with the addition of PAC and APAM, to investigate the performance of ANN in predicting phosphorous adsorption, and to model isotherm adsorption, kinetics, and thermodynamics by using an index of model performance for probing the potential adsorption mechanisms.

MATERIALS AND METHODS

WTRs sampling and preparation

Air-dried WTRs cakes were sampled from a drinking water treatment plant with a treatment capacity of 800,000 m^3/day in Taiyuan city, Shanxi Province, China. In the water treatment plant, raw surface water mixed with PAC goes through sedimentation, filtration, and disinfection units, and finally becomes distributed drinking water. WTRs mainly come from the sedimentation basins that flow into gravity thickening basins after mixing with APAM in the collection and distribution tanks. The water then subsequently flows into equalization tanks, is dewatered by plate and frame filter presses after adding APAM again, and ultimately

becomes sludge cakes after air drying so it is ready for transportation to a landfill. The WTRs cakes were transported into the lab, and immediately further dried at 105 °C for one hour. The samples were ground, passed through a 0.25-mm mesh sieve, and sealed and stored in glass bottles at room temperature for use in the P adsorption experiments.

Aqueous solutions

Two types of aqueous solutions were employed in the study. One is a distilled de-ionized (DDI) water solution with different predesigned P concentrations, while the other is an artificial stormwater with different predesigned P concentrations. The artificial stormwater was made similarly to the method provided by Blecken *et al.* (2010). In addition to phosphorus, NH_4^+-N, NO_x-N, Organic-N, and COD were included at concentrations of 5 mg/L, 4 mg/L, 0.5 mg/L, and 80 mg/L, respectively, with a pH of 7. The aqueous solutions were made with laboratory-grade chemicals and DDI water.

P adsorption studies

Batch experiments were performed for P isotherm adsorption models, adsorption kinetics models, and a thermodynamic model. WTRs samples with 100 mL of a P-containing aqueous solution at a predesigned pH were filled in 250-mL flask bottles and shaken by a rotary shaker at 140 r/min and at a predesigned temperature. The solution pH was adjusted by adding 0.1 M HCl or 0.1 M NaOH. The solution samples were taken at a time after the start of the adsorption reaction, centrifuged at 3,000 r/min, and filtered with 0.45-μm syringe filters for P analysis using the standard ascorbic acid method (Baird *et al.* 2017). There were three replications for each test. The adsorption removal ratio was determined by Equation (1).

$$ARR_t = \frac{C_0 - C_t}{C_0} \times 100 \tag{1}$$

where ARR_t (%) is the adsorption removal ratio at t (time), and C_0 (mg/L) and C_t (mg/L) are the initial P concentration and the P concentration at time, t, in the aqueous solution, respectively.

Prior to modeling studies, data were obtained by batch experiments including the aqueous solution category, either P in DDI water or P in artificial stormwater, at initial concentrations, $C_{0,}$ of 10, 20, 40, 60, 80, and 100 mg/L, pH of 5, 6, 7, 8, and 9, time at 0.25, 0.50, 0.75, 1.00, 1.50, 2.00, 2.50, 3.00, and 24.00 hours, temperature of 20, 30, and 40 °C, WTRs dosage of 6, 8, 10, 12, and 14 g/L, C_t, adsorbed P onto WTRs (mg/g) at t, and the respective calculated ARR_t. Adsorbed P onto WTRs was calculated by Equation (2).

$$C_{st} = \frac{C_0 - C_t}{m} \times V \tag{2}$$

where C_{st} is adsorbed P by WTRs (mg P/g) at t, m is the WTRs dosage (g), and V is the solution volume (L).

Statistical analysis and index of model performance

The language R was employed to conduct the statistical analysis and complete the modeling (R Core Team 2019). A paired t-test was used to compare the difference of C_t at the p-value <0.05 level between two solutions under the same conditions.

The adsorption models were evaluated by comparing the difference between predicted and measured values. The index of model performance encompassed the sum of squared error (*SSE*), coefficient of determination (R^2), adjusted R^2, model efficiency (*EF*, %), mean error (*ME*), and root of the mean square error (*RMSE*).

SSE is the difference between the measured value and the predicted value for a specific model. It has been used by researchers to compare or evaluate model performance. *SSE* is shown in Equation (3), where i is the number of the i-th adsorption measurement, n is the total number of measurements, $A(m)_i$ is the i-th measured value, and $A(p)_i$ is the i-th value predicted by the model. A lower *SSE* of a model means better performance (Duan *et al.* 2011).

$$SSE = \sum_{i=1}^{n} (A(m)_i - A(p)_i)^2 \tag{3}$$

R^2 can illustrate the proportion of the total variability of the fitted non-linearized or linearized models. However, since the drawback of using R^2 is that it can be higher by increasing the number of independent variables during the modeling, an adjusted R^2 is used as an alternative index

(Duan *et al.* 2011). Adjusted R^2 partially depends on the degree of freedom that is determined by the independent variable number and the number of observations in a set of adsorption measurements. The minimum and maximum value of R^2 and adjusted R^2 are zero and one, respectively for both variables. If R^2 and adjusted R^2 are one, it means that the model perfectly fits the data.

Model efficiency (*EF*) is another model index to evaluate goodness of fit by a model (Duan *et al.* 2011). It can be calculated by Equations (4) and (5). The term $\overline{A(m)_i}$ is the average value of the measurements. When *EF* is a negative value, *EF* is set to zero. As a result, *EF* ranges from 0 to 100. Higher *EF* for a model means better agreement between measured and predicted values (Duan *et al.* 2011).

$$EF = \left(1 - \frac{SSE}{D_0}\right) \times 100 \tag{4}$$

$$D_0 = \sum_{i=1}^{n} (A(m)_i - \overline{A(m)_i})^2 \tag{5}$$

The mean error (*ME*) and the root of the mean square error (*RMSE*) were used to analyze the residual and are defined by Equations (6) and (7), respectively (Duan *et al.* 2011). $I(p)_j$ is the model predicted value; $I(m)_j$ is the measured value in the adsorption studies; j is the number of the j-th adsorption measurement; and n is the total number of adsorption measurements. The *ME* statistic is used to indicate whether the model overestimates or underestimates the measured adsorption values as a whole (Duan *et al.* 2011). Mathematically, *RMSE* is larger than zero and can be zero, but that rarely happens in practice. If one model's *RMSE* is closer to zero than others, it means that this model is better than the others in terms of *RMSE* (Duan *et al.* 2011).

$$ME = \sum_{j=1}^{n} \frac{I(p)_j - I(m)_j}{n} \tag{6}$$

$$RMSE = \sqrt{\frac{\sum_{j=1}^{n} (I(p)_j - I(m)_j)^2}{n}} \tag{7}$$

Isotherm adsorption models

The Langmuir model (Equation (8)) and Freundlich model (Ng *et al.* 2002) (Equation (9)) were utilized to fit the isotherm adsorption data.

$$q_e = \frac{q_m b C_e}{1 + bC_e} \tag{8}$$

$$q_e = K_F C_e^{1/n} \tag{9}$$

where q_e is the P adsorption capacity at equilibrium per unit mass of WTRs (mg/g), C_e (mg/L) is the equilibrium P concentration, q_m (mg/g) is the maximum P adsorption capacity of WTRs, and b (L/mg) is the Langmuir isotherm constant; K_F ($mg^{(1-1/n)}L^{1/n}$ /g)) and n are the Freundlich isotherm constants.

Adsorption kinetics models

Three different adsorption kinetics models were used to describe the relationship of P adsorption onto WTRs with time including the pseudo first-order model (Ho & McKay 1999) (Equation (10)), pseudo second-order model (Ho 2006) (Equation (11)), and intraparticle diffusion model (Ho & McKay 1998) (Equation (12)).

$$q_t = q_e(1 - e^{-k_1 t}) \tag{10}$$

$$q_t = \frac{q_e^2 k_2 t}{1 + q_e k_2 t} \tag{11}$$

$$q_t = K_P t^{1/2} + C \tag{12}$$

where q_t (mg/g) is the P adsorption at time t per unit mass of WTRs; k_1 (1/hr), k_2 (g/(mg·hr)) and K_P (mg/(g·$hr^{1/2}$)) are the rate constants; and C (mg/g) is a constant.

Thermodynamic analysis

Adsorption thermodynamic analysis can be used to deduce the type of adsorption process at a given temperature under reaction conditions. The values of the thermodynamic parameters including free energy (ΔG^o, J/mol), enthalpy (ΔH^o, J/mol), and entropy (ΔS^o, J/mol/K) are indicators of the type of adsorption process. These three parameters were calculated by using the following three equations (Equations (13)–(15)) (Khan *et al.* 2017). The data used for these calculations were the amount of P adsorption onto

WTRs at equilibrium at temperatures of 20, 30, and 40 °C.

$$K_d = \frac{C_0 - C_e}{C_e} \times \frac{V}{m} \tag{13}$$

$$\Delta G^\circ = -RTlnK_d \tag{14}$$

$$lnK_d = \frac{\Delta S^\circ}{R} - \frac{\Delta H^\circ}{RT} \tag{15}$$

where K_d is the distribution coefficient (L/g); R is the universal gas constant (8.314 J/mol/K); and T is the adsorption temperature (K).

ANN models

Generally, the architecture of ANN models encompasses an input layer with l neurons, hidden layer with m neurons, and output layer with n neurons. In this study, the neurons in the input layer included ($l = 4$) initial P concentration (C_0) in solution, the dosage of WTR, pH, and adsorption time, and the output layer had one neuron ($n = 1$) that was the P concentration (C_t) in solution at time t. The number of neurons in the hidden layer was determined by the optimization process of the ANN models (Ciaburro & Venkateswaran 2017). Weighted values from the input layer for input values in each neuron are transferred into the hidden layer. Each neuron in the hidden layer processes the sum of the weighted values from the input layer and transfers the result to the neuron in the output layer, as shown in Figure 1 (x_i is the i-th neuron; w_i is the i-th weight, and f is a non-linear function called the activation function). The processing completed by a neuron in the hidden layer can be expressed by Equation (16) (Ciaburro & Venkateswaran 2017).

$$\text{output} = f(\text{sum}(\text{weights} \times \text{inputs})) + \text{bias} \tag{16}$$

Weights and bias are two important numerical parameters. Weights show the strength of one neuron impacting the other neuron (Ciaburro & Venkateswaran 2017). Bias is an additional parameter used to adjust the output (Ciaburro & Venkateswaran 2017).

The R package neuralnet (Fritsch *et al.* 2019; R Core Team 2019) was employed to construct the ANN models in the study. The training of ANN models was conducted by supervised learning by providing the neural network with inputs and the measured outputs. The 72 sets of adsorption data were randomly split into a training dataset and a testing dataset in the ratio of 70%–30%. Prior to the training of a neural network, the data were normalized by using the min-max method (also called feature scaling method, see Equation (17)) to have all the scaled data in the range of 0–1 with an aim of eliminating the impacts of data units in algorithm convergence (Ciaburro & Venkateswaran 2017).

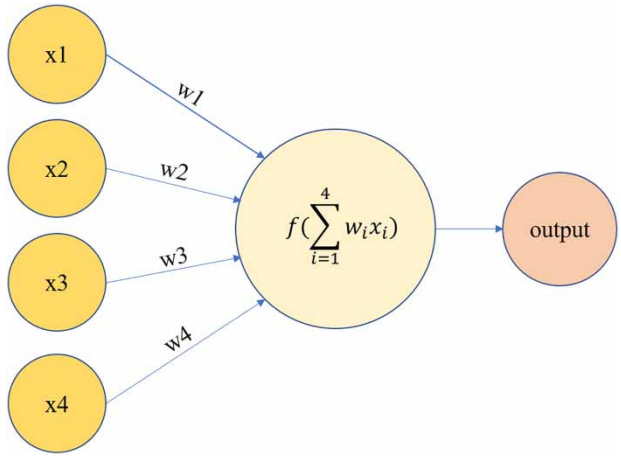

Figure 1 | The process of a neuron in the hidden layer.

$$x_{scaled} = \frac{x - x_{min}}{x_{max} - x_{min}} \tag{17}$$

where x_{scaled} is the scaled value of an input value of a variable; x_{min} or x_{max} is the minimum or maximum value of all input values of a variable.

ANN model training was accomplished by feeding training data into the R package neuralnet. The activation function was the logistic function, the error function was the sum of squared errors (*SSE*), and the algorithm type for calculating the neural network was resilient backpropagation with weight backtracking (Fritsch *et al.* 2019). To avoid the problem of overfitting, the number of neurons (m) in the hidden layer was selected in the range from 2 to 10 based on rules of thumb (Ciaburro & Venkateswaran 2017). After the training phase, the obtained ANN model went into the testing phase, and its performance was evaluated by using testing data to check the difference between

the predicted output and the actual output. For the final deployment of the ANN model, the m value required optimization. The optimized m value was determined by evaluating performances of the trained models with different m values by comparing mean standard error (*MSE*) (Equation (18)) and Pearson's determination coefficient (R^2) (Equation (19)).

$$\mathrm{MSE} = \frac{1}{n}\sum_{i=1}^{n}(C_{t,\,predict} - C_{t,measurment})^2 \tag{18}$$

$$R^2 = \frac{\left[\sum_{i=1}^{n}(C_{t,predict} - \bar{C}_{t,predict})(C_{t,measurement} - \bar{C}_{t,measurement})\right]^2}{\sum_{i=1}^{n}(C_{t,predict} - \bar{C}_{t,predict})^2 \sum_{i=1}^{n}(C_{t,measurement} - \bar{C}_{t,measurement})^2} \tag{19}$$

In Equations (18) and (19), n is the total number of observations, $\bar{C}_{t,predict}$ and $\bar{C}_{t,measurement}$ are the average values of the predicted and measured values of C_t, respectively.

RESULTS AND DISCUSSION

Characterization of WTRs

The bulk density of the WTRs used in these tests was 1.144 g/cm^3. The element analysis showed that the WTRs contained 11.38% carbon, 0.95% nitrogen, 2.90% hydrogen, 34.43% oxygen, 0.35% sulfur, 7.16% Al, 0.37% Fe, 1.92% Ca, and 0.20% Mg. The pH is 7.6 at a ratio of soil to water of 1:1 (m/v). BET surface area, t-Plot micropore volume, single point adsorption total pore volume of pores, and adsorption average pore width of WTRs were 36.6934 m^2/g, 0.001262 cm^3/g, 0.062340 cm^3/g, and 6.79572 nm, respectively. Scanning electron micrograph of WTRs illustrated that the WTRs had an irregular surface with macro-pores and micro-pores possibly impacting the adsorption of phosphorus.

ANN models

After many adjustments of the ANN model parameter, m, by comparing *MSE* and R^2 values, the hidden layer neuron number was finally determined by selecting the minimum *MSE* value and maximum R^2. ANN models for P adsorption by WTRs in a DDI water solution ($m = 8$) and stormwater solution ($m = 6$) are shown in Figures 2 and 3. The *MSE* of ANN in the DDI water solution and stormwater solution was 0.018 and 0.053, respectively, and the R^2 of ANN in a DDI water solution and stormwater solution was 0.999 and 0.998, respectively.

In both figures, error (*SSE*) was automatically calculated by the R package based on the normalized input values of initial P concentration, pH, adsorption time, and WTRs dosage. Steps means the total number of the training set of

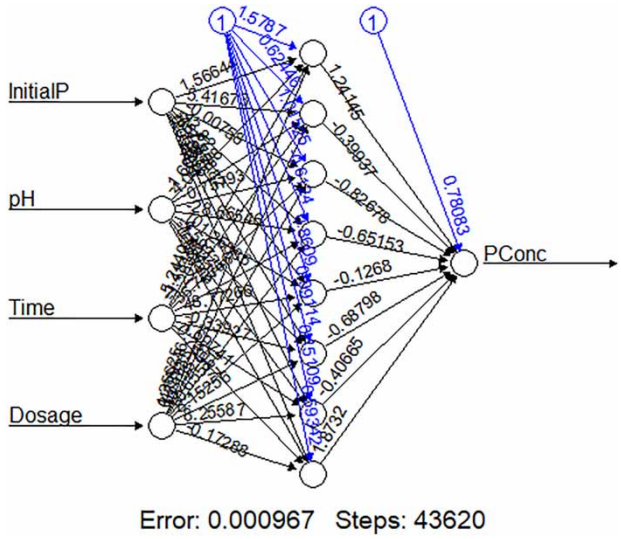

Figure 2 | ANN model for P adsorption by WTRs in DDI water solution.

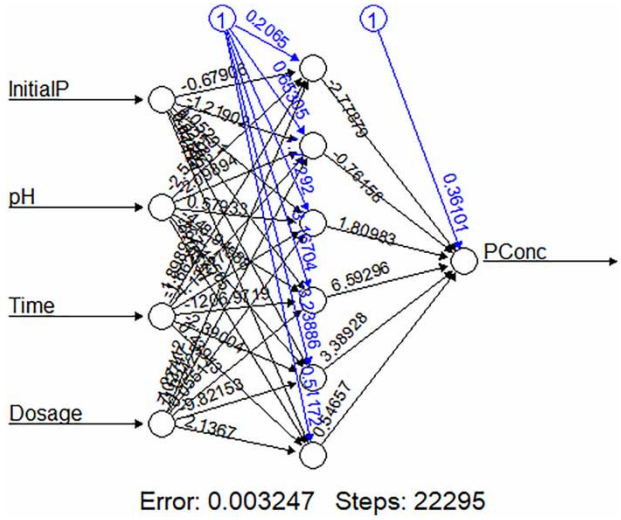

Figure 3 | ANN model for P adsorption by WTRs in stormwater solution.

the neural network model, the values on lines from 1 to neuron are the errors, and the values on the lines connecting neurons are weights.

Effects of WTRs dosage

The adsorbent dosage is one of the important adsorption parameters that impacts adsorption capacity and adsorption equilibrium at a given adsorbate concentration. The optimum WTRs dosage was determined as 10 g/L in both solutions (Figure 4). Paired t-test showed that P concentration after 24-hour adsorption by WTRs in stormwater was significantly higher than in the DDI solution (P-value = 0.02146 < 0.05) with a pH of 7, initial P concentration of 20 mg/L, and temperature of 30 °C. The P concentration in both solutions after 24 hours of adsorption decreased with WTRs dosage increasing from 6 to 10 g/L (Figure 4) due to increased surface area and more adsorption sites. Less P adsorption from the stormwater compared to the DDI water solution may be caused by competition and influence of other ions or compounds in the stormwater. Krishna *et al.* (2016) claimed that the competitive ions included nitrate ions along with chloride, carbonate, and sulfate ions. In addition to nitrate ions, stormwater solutions contain organic-N and other organics.

The P adsorption ARR_t after 24 hours with WTR dosages of 6, 8, 10, 12, and 14 g/L was 77.23, 91.30, 99.58, 100, and 100% in the DDI water solution, and 72.82, 87.62, 100, 100, and 100% in the stormwater solution, respectively. The ANN model predicted P adsorption ARR_t after 24 hours of adsorption with dosages of 6, 8, 10, 12, and 14 g/L was 77.24, 91.91, 100, 100, and 100% in DDI water solution, and 72.84, 87.55, 99.99, 100, and 100% in stormwater solution, respectively. The ANN model predictions in terms of the effects of WTRs dosage (Figure 4) were in good agreement with the experimentally measured results.

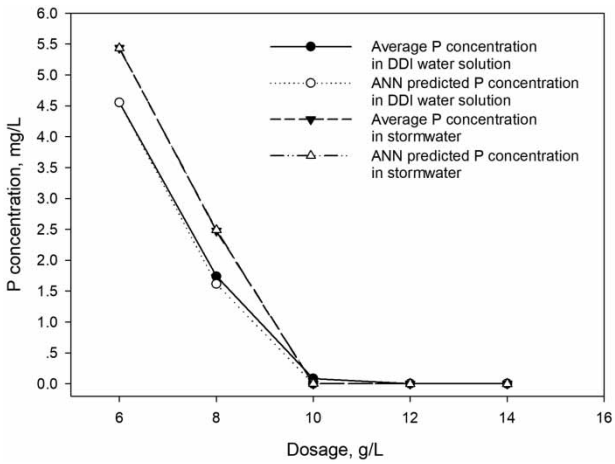

Figure 4 | WTRs dosage effects on P adsorption (t = 24 hours, pH = 7, initial P concentration = 20 mg/L, and temperature = 30 °C).

Effects of pH

An important parameter used to measure the adsorption process is pH since its variance can change adsorbent surface characteristics and subsequently influence adsorption capacity. In addition, P adsorption onto WTRs is possibly partially controlled by ligand exchange between P in solution and -OH on the WTRs surface (Krishna *et al.* 2016). The results confirmed that P adsorption decreased with the increase of solution pH, which is similar to Ippolito *et al.* (2011). Similar to effects of dosage on P concentration, paired t-test showed that the P concentration after a 24-hour adsorption period by the WTRs in stormwater was significantly higher than that found in the DDI solution (P-value = 0.00003< 0.05) with a dosage of 6 g/L, initial P concentration of 20 mg/L, and temperature of 30 °C and in the common range of stormwater pH from 5 to 9. The optimum pH was 5 in the range of 5–9 in both solutions, but it was 6 for groundwater treatment plant sludges in the range of 4–9 (Krishna *et al.* 2016). It shows that the optimum pH for P adsorption is related to the water source, formation, characteristics, and compounds of the WTRs. For engineering application, the mechanisms should be further probed on the influence of other ions, compounds and characteristics over a range of pH.

Experimental measured and ANN model predicted P concentration after 24 hours increased with an increase in the water source pH from 5 to 9 in both solutions (Figure 5). The P adsorption ARR_t after 24-hour with pH of 5, 6, 7, 8, and 9 was 82.22%, 75.08%, 70.83%, 66.75%, and 62.57% in DDI water solution, and 75.08%, 70.88%, 68.25%, 64.17%, and 61.72% in stormwater solution, respectively. The ANN model predicted P adsorption ARR_t after 24-hour adsorption with pH of 5, 6, 7, 8, and 9 was 82.22%, 75.25%, 70.81%, 67.66%, and 62.42% in DDI water solution, and 75.09%, 71.12%, 69.03%, 65.60%, and 61.50% in stormwater solution,

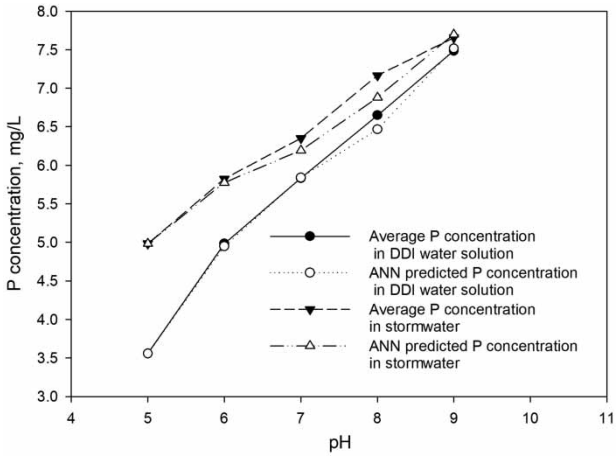

Figure 5 | Solution pH effects on P adsorption (t = 24 hours, dosage = 6 g/L, initial P concentration = 20 mg/L, and temperature = 30 °C).

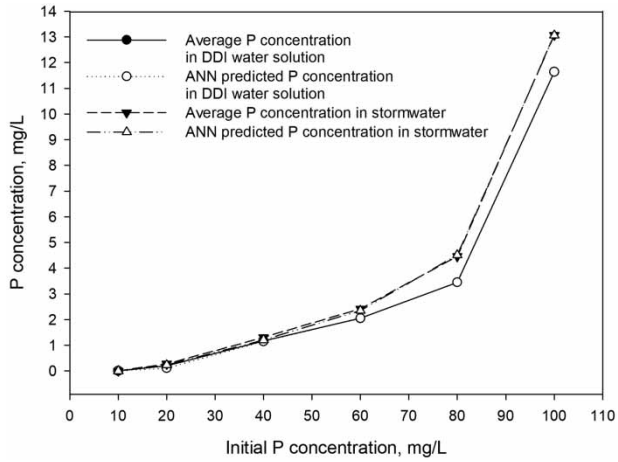

Figure 6 | Initial P concentration effects on P adsorption (t = 24 hours, dose = 10 g/L, pH = 5, and temperature = 30 °C).

respectively. The ANN model predictions in terms of the effects of solution pH (Figure 5) were in good agreement with the experimental measured results.

Effects of initial P concentration

As an important parameter, initial P concentration (C_0) provides the initial adsorbate concentration gradient as the mass transfer driving force. The result of the paired t-test is that final P concentration with different initial P concentration after 24-hour of adsorption in stormwater was significantly (P-value = 0.00154 < 0.05) higher than in DDI water solution with dose of 10 g/L, pH of 5, and temperature of 30 °C (Figure 6).

The experimental measured and ANN model predicted P adsorption ARR_t after 24 hours with initial P concentrations of 10, 20, 40, 60, 80, and 100 mg/L in DDI solutions was 100, 99.01, 94.15, 89.74, 82.77, and 41.84, and 100, 99.47, 94.22, 89.73, 82.77, and 41.84%, respectively. The experimental measured and ANN model predicted P adsorption ARR_t after 24 hours with initial P concentrations of 10, 20, 40, 60, 80, and 100 mg/L in stormwater was 100, 98.61, 93.45, 87.89, 77.70, and 34.67, and 100, 98.81, 93.96, 88.25, 77.44, and 34.70%, respectively. ANN model predictions are in good agreement with experimental measured values in DDI water solution and stormwater. In addition, P concentration after 24-h adsorption increased and the adsorption removal ratio decreased with the increase in initial P concentration. The higher ARR_t at lower C_0 was possibly caused by relatively more adsorption sites available than P ions while the lower ARR_t may be due to relatively less or insufficient adsorption sites available for relatively more P ions for adsorption.

Isotherm adsorption

Adsorption isotherms can be used to investigate adsorption mechanisms. The parameters of isotherm adsorption models, the Langmuir model and Freundlich model, were initially determined by curve fitting the linearized equations of both models by using the experimental measured values of q_e and C_e so that both isotherm adsorption models could be constructed. The linearized equations of the Langmuir and Freundlich models are shown as Equations (20) and (21), respectively.

$$\frac{C_e}{q_e} = \frac{1}{bq_m} + \frac{C_e}{q_m} \tag{20}$$

$$lnq_e = lnK_F + \frac{1}{n} lnC_e \tag{21}$$

Although most of isotherm adsorption studies adopted the above linearized approach to calculate the parameters of the isotherm adsorption models, the parameters can be determined by modern computing software or programs such as R, Origin, or self-written codes in various programming environments on different operating systems. The parameters resulting from direct curve fitting of non-linearized models

are different from those obtained from an indirect method under optimum conditions: pH = 5, temperature = 30 °C, dose = 10 g/L, time = 24 hours, and initial P concentration = 10, 20, 40, 60, 80, and 100 mg/L. The reason is that the transformation of non-linear models to linear models may change the error structures and possibly even results in violating assumptions of normality and error variance in using a standard least-square approach during linear regression for linearized models (Hamdaoui & Naffrechoux 2007).

The parameters of the Langmuir model determined by linearized and non-linearized curve fitting were: q_m = 9.398 mg/g (linearized) and 10.118 mg/g (non-linearized) in the DDI water solution, and 9.285 mg/g (linearized) and 9.955 mg/g (non-linearized) in the stormwater solution. The b value was 1.150 L/mg (linearized) and 0.684 L/mg (non-linearized) in the DDI water solution, and 0.958 L/mg (linearized) and 0.585 L/mg (non-linearized) in the stormwater solution. The parameters of the Freundlich model determined by linearized and non-linearized curve fitting were: K_F, 3.939 $mg^{(1-1/n)}L^{1/n}/g$ (linearized) and 4.313 $mg^{(1-1/n)}L^{1/n}/g$ (non-linearized) in DDI water solution, and 3.570 $mg^{(1-1/n)}L^{1/n}/g$ (linearized) and 3.978 $mg^{(1-1/n)}L^{1/n}/g$ (non-linearized) in stormwater. The value for n is 2.554 (linearized) and 3.148 (non-linearized) for the DDI water solution, and 2.458 (linearized) and 3.037 (non-linearized) for the stormwater solution.

After transformation of non-linear models, the linearized models in reality describe the relationship of C_e/q_e (y) and C_e (x), and lnq_e (y) and lnC_e (x), respectively. The R^2 obtained during linear regression only reflects the relationship of C_e/q_e (y) and C_e (x), and lnq_e (y) and lnC_e (x), respectively. The values for q_m and K_F obtained from curve fitting non-linearized models were higher than linearized models. These values imply that both parameters should be determined by non-linearized curve fitting rather than linearized curve fitting if higher accuracy is required.

For comparing the prediction ability of the three models tested, *SSE*, R^2, *adj.* R^2, *EF*, *ME*, and *RMSE* of Langmuir model and Freundlich model were calculated by using parameters obtained from direct and indirect curve fitting (Table 1). For P adsorption in both solutions, the non-linearized Langmuir model had better prediction than the linearized Langmuir model since R^2, *adj.* R^2, and *EF* of the former were higher than the latter, and *SSE*, the absolute value of *ME*, and *RMSE* of the former were lower than the latter (Table 1). The negative value of *ME* showed that the non-linearized Langmuir model underestimated the measured adsorption values as a whole in both solutions (Table 1). Linearized and non-linearized models had positive *ME* values, meaning that they over-estimated the measured adsorption values in the other cases (Table 1). Although the *ME* values of non-linearized Freundlich models were higher than linearized Freundlich models in both solutions, the values of the other five indexes of model performance indicated that non-linearized Freundlich models had better prediction of P adsorption in both solutions (Table 1). Meanwhile, overall, the non-linearized Langmuir model was better than the non-linearized Freundlich model for P adsorption prediction (Table 1). Although WTRs used in this study were different from other studies as they notably contained PAC and APAM, the adsorption isotherms fitted the Langmuir model better than the Freundlich model, as similarly reported by other studies (Babatunde & Zhao 2010; Krishna *et al.* 2016). The results show that the P adsorption onto WTRs was monolayer with the WTRs surface having homogenous active sites possessing the same and constant energy.

The dimensionless equilibrium parameter, R_L, is often used to indicate the favorable nature of adsorption (Kilic

Table 1 | Index of model performance of linearized Langmuir model (1), non-linearized Langmuir model (2), linearized Freundlich model (3), and non-linearized Freundlich model (4)

Solution	Model	SSE	R^2	Adj. R^2	EF	ME	RMSE
DDI	1	3.013	0.924	0.899	90.214	0.369	0.776
	2	1.309	0.964	0.952	95.749	−0.087	0.512
	3	4.155	0.889	0.852	86.503	0.008	0.912
	4	2.851	0.910	0.880	90.739	0.036	0.755
Stormwater	1	2.231	0.950	0.933	92.455	0.378	0.668
	2	0.682	0.980	0.974	97.693	−0.059	0.369
	3	3.579	0.905	0.873	87.893	0.019	0.846
	4	2.256	0.926	0.901	92.371	0.043	0.672

et al. 2011). $R_L = 1/(1 + bC_0)$, where b is the Langmuir constant and C_0 is the initial adsorbate concentration in solution. $R_L = 0$ means the isotherm adsorption is irreversible, $R_L = 1$ linear, $R_L > 1$ unfavorable, or $1 > R_L > 0$ favorable. Since all values of b and C_0 were larger than 0 in the study, all values of R_L fell into the range of 0–1, showing that the isotherm adsorption was favorable. All Freundlich parameter n were larger than 1, so that $1/n$ was less than 1, also indicating that the isotherm adsorption was favorable.

Previous studies indicate that P adsorption capacity by WTRs was 0.424 mg P/g (Mortula & Gagnon 2007), 0.7–3.5 mg P/g (Yang *et al.* 2006), 6.3–10.2 mg P/g (Razali *et al.* 2007), 10.2–31.9 mg P/g (Babatunde & Zhao 2010), 32.27–47.62 mg P/g (Krishna *et al.* 2016), and 4.167–90.909 mg P/g (Li *et al.* 2013) depending on different alum based WTRs and experimental conditions. The maximum adsorption capacity (q_m) of WTRs containing PAC and APAM was determined to be 10.118 mg P/g WTRs in DDI water solution and 9.955 mg P/g WTRs in stormwater solution by using non-linearized Langmuir model. It can be seen that the maximum adsorption capacity of WTRs used in this study was significant compared with soils (0.93 mg P/g) (Babatunde & Zhao 2010) and comparable to previous similar studies. Therefore, the WTRs used in this study could be a candidate as the media or substrate in a stormwater bioretention system in terms of P removal.

P adsorption kinetics by WTRs

The non-linearized pseudo first-order model, pseudo second-order model, and intraparticle diffusion model were directly curve fitted with the experimental measured data. Their parameters were obtained under the following conditions: pH = 5, temperature = 30 °C, dose = 10 g/L, initial P concentration = 20 mg/L and time = 0.25, 0.50, 0.75, 1.00, 1.50, 2.00, 2.50, and 3.00 hours. The parameters of the pseudo first-order model were: q_e, 1.922 mg/g, k_1, 1.770/hour in DDI water solution and q_e, 1.899 mg/g, k_1, 2.236/hour in stormwater. The parameters of pseudo second-order model were: q_e, 2.271 mg/g, k_2, 0.946 g/mg/hour in DDI water solution and q_e, 2.193 mg/g, k_2, 1.318 g/mg/hour in stormwater. The experimentally measured q_e was 1.999 for both solutions. The parameters of the intraparticle model were: $K_P = 1.119$ mg/g/hour$^{1/2}$, $C = 0.256$ mg/g in DDI water solution and $K_P = 1.092$ mg/g/hour$^{1/2}$, $C = 0.339$ mg/g in stormwater.

Performance indexes of these three models are listed in Table 2 for the P adsorption for both solutions. The pseudo second-order model was notably better than the other two models since *SSE*, the absolution value of *ME*, and *RMSE* of the pseudo second-order model are smaller than the other models while its R^2, *adj.* R^2, and *EF* are larger (Table 2) for both solutions. The negative values of *ME* indicated that all three models underestimated the measured values.

In reality, three adsorption kinetics models can be well fitted with R^2 higher than 0.9 by P adsorption experimental data. As in previous studies, the pseudo second-order model had the best fit (Babatunde & Zhao 2010). Krishna *et al.* (2016) found that the pseudo first-order model had higher R^2, but they thought that P adsorption onto WTRs should comply with the pseudo second-order model because this had a lower difference between experimental q_e and q_e determined by data fitting (Krishna *et al.* 2016). P adsorption was in agreement with the pseudo second-order model, indicating that it was controlled by the chemisorption process (Kilic *et al.* 2011). The intercept (C) was higher than zero, showing that intraparticle diffusion was controlled by boundary layer effects to some extent and not only the rate-limiting step (Babatunde & Zhao 2010; Kilic *et al.*

Table 2 | Performance indexes of models: pseudo first-order model (1), pseudo second-order model (2), and intraparticle diffusion model (3)

Solution	Model	SSE	R^2	Adj. R^2	EF	ME	RMSE
	1	0.129	0.960	0.954	88.208	−0.015	0.127
DDI water	2	0.054	0.983	0.981	95.096	−0.004	0.082
	3	0.098	0.949	0.942	91.007	−0.033	0.111
	1	0.107	0.967	0.962	88.065	−0.010	0.115
Stormwater	2	0.033	0.990	0.988	96.270	−0.002	0.065
	3	0.171	0.911	0.898	80.886	−0.043	0.146

2011). P adsorption may be affected by multiple kinetic processes, and possibly at least simultaneously contains surface adsorption and intraparticle diffusion.

Adsorption thermodynamics

Adsorption thermodynamics can be used to judge whether the adsorption reaction could occur at some range of temperatures during practical engineering applications. The adsorption distribution coefficient, K_d, was 3.377 ± 0.027, 5.998 ± 0.065, and 12.847 ± 0.215 L/g at temperatures of 20, 30, and 40 °C with initial P concentration of 20 mg/L, pH of 5, WTRs dosage of 10 g/L, and adsorption time of 24 hours in DDI water solutions, and 3.089 ± 0.289, 5.773 ± 0.946, and 12.718 ± 0.722 L/g at temperatures of 20, 30, and 40 °C in stormwater solutions, respectively. Gibbs free energy, ΔG^o, was −2.964, −4.513, and −6.644 kJ/mol at temperatures of 20, 30, and 40 °C in DDI water solutions, and −2.747, −4.417, and −6.618 kJ/mol at temperatures of 20, 30, and 40 °C in stormwater solutions, respectively. ΔH^o and ΔS^o were calculated from the slope and the intercept of the straight line obtained by curve fitting of lnK_d versus $1/T$. The R^2 of the straight lines was 0.9901 in DDI water solution and 0.9926 in stormwater. ΔH^o *and* ΔS^o were 50.843 kJ/mol and 183.332 J/mol/K in DDI water solution, and 53.863 kJ/mol and 192.926 J/mol/K for stormwater, respectively. Negative Gibbs free energy values indicate that the adsorption of P by WTRs is a spontaneous process in both solutions in the range of experimental temperatures. Positive values of ΔH^o show that the P adsorption by WTRs is an endothermic process in both solutions in nature. Also, positive values of ΔS^o indicate that the P adsorption by WTRs is an entropy production process for both solutions.

CONCLUSIONS

This study demonstrates that air-dried WTRs containing PAC and APAM from sludge dewatering units of a typical water treatment facility, a type of WTRs found world-wide and recently available, can be effectively reused as a potential alternative part of traditional soil-based media or substrate in stormwater bioretention systems for P removal from stormwater runoff. The outcomes are listed below:

(1) ANN models can accurately predict the P concentration at equilibrium in solutions in the WTRs adsorption process. Therefore, once sufficient data are available for constructing robust ANN models in engineering practices, ANN models will be important tools for environmental professionals to control non-point source P pollution by natural treatment systems in the future in a sustainable manner.
(2) Non-linearized Langmuir model fitted the isotherms data better than others with q_m of 10.118 and 9.955 mg/g in DDI solution and stormwater, respectively. The P adsorption onto WTRs is a homogenous monolayer adsorption and a favorable process.
(3) Pseudo second-order kinetic model predicted experimental data better than the pseudo first-order and intraparticle diffusion models. The adsorption process may be controlled by multiple kinetic processes or at least surface adsorption and intraparticle may diffuse simultaneously.
(4) The P adsorption onto WTRs is a spontaneous, endothermic, and entropy production process.
(5) Air-dried WTRs containing PAC and APAM were found to be effective in removing P from DDI water solution and stormwater, but the P removals at equilibrium had significant differences.

Different types of WTRs originated from the different water treatment processes used around the world with different coagulants having been proven to have different P adsorption capacity and adsorption mechanisms. For better management and reuse of the type of waste used in this study, further research should be performed on the competitive adsorption mechanisms and models between the P ion and other ions or compounds in solutions, on the dynamic P adsorption mechanisms in the flows through WTRs layers, and on the P adsorption mechanisms influenced by PAC and APAM in WTRs. Also, the P adsorption capacity of more WTRs of different particle sizes should be further investigated for PAC-APAM WTRs.

ACKNOWLEDGEMENT

This work was supported by a new faculty startup fund provided by Taiyuan University of Technology, China and by the Natural Science Foundation of Shanxi Province, China

(201901D111068). The funding agencies had no involvement in the research and the preparation of the article.

DATA AVAILABILITY STATEMENT

All relevant data are included in the paper or its Supplementary Information.

REFERENCES

Abba, S. I. & Elkiran, G. 2017 Effluent prediction of chemical oxygen demand from the wastewater treatment plant using artificial neural network application. *Procedia Computer Science* **120**, 156–163.

Al-Tahmazi, T. & Babatunde, A. O. 2016 Mechanistic study of P retention by dewatered waterworks sludges. *Environmental Technology & Innovation* **6**, 38–48.

Babatunde, A. O. & Zhao, Y. Q. 2010 Equilibrium and kinetic analysis of phosphorus adsorption from aqueous solution using waste alum sludge. *Journal of Hazardous Materials* **184**, 746–752.

Babatunde, A. O., Zhao, Y. Q., Burke, A. M., Morris, M. A. & Hanrahan, J. P. 2009 Characterization of aluminum-based water treatment residual for potential phosphorus removal in engineered wetlands. *Environmental Pollution* **157**, 2830–2836.

Baird, R. B., Eaton, A. D. & Rice, E. W. 2017 *Standard Methods for the Examination of Water and Wastewater*, 23rd edn. American Water Works Association/Water Environment Federation/American Public Health Association, Washington, DC, USA.

Blecken, G. T., Zinger, Y., Deletić, A., Fletcher, T. D., Hedström, A. & Viklander, M. 2010 Laboratory study on stormwater biofiltration: nutrient and sediment removal in cold temperatures. *Journal of Hydrology* **394**, 507–514.

Ciaburro, G. & Venkateswaran, B. 2017 *Neural Networks with R*. Packt Publishing Ltd, Birmingham, UK.

Dassanayake, K. B., Jayasinghe, G. Y., Surapaneni, A. & Hetherington, C. 2015 A review on alum sludge reuse with special reference to agricultural applications and future challenges. *Waste Management* **38**, 321–335.

Duan, R., Fedler, C. B. & Borrelli, J. 2011 Field evaluation of infiltration models in lawn soils. *Irrigation Science* **29**, 379–389.

Fritsch, S., Guenther, F. & Wright, M. N. 2019 *neuralnet: Training of Neural Networks*. R package version 1.44.2. Available from: https://CRAN.R-project.org/package=neuralnet (accessed 22 October 2019).

Hamdaoui, O. & Naffrechoux, E. 2007 Modeling of adsorption isotherms of phenol and chlorophenols onto granular activated carbon: part I. Two-parameter models and equations allowing determination of thermodynamic parameters. *Journal of Hazardous Materials* **147**, 381–394.

Ho, Y. S. 2006 Review of second-order models for adsorption systems. *Journal of Hazardous Materials* **136**, 681–689.

Ho, Y. S. & McKay, G. 1998 Sorption of dye from aqueous solution by peat. *Chemical Engineering Journal* **70**, 115–124.

Ho, Y. S. & McKay, G. 1999 Pseudo-second order model for sorption processes. *Process Biochemistry* **34**, 451–465.

Ippolito, J. A., Barbarick, K. A. & Elliott, H. A. 2011 Drinking water treatment residuals: a review of recent uses. *Journal of Environment Quality* **40**, 1–12.

Khan, T., Mustafa, M. R. U., Isa, M. H., Manan, T. S. B. A., Ho, Y. C., Lim, J. W. & Yusof, N. Z. 2017 Artificial neural network (ANN) for modelling adsorption of lead (Pb (II)) from aqueous solution. *Water, Air, & Soil Pollution* **228**, 426–440.

Kilic, M., Apaydin-Varol, E. & Pütün, A. E. 2011 Adsorptive removal of phenol from aqueous solutions on activated carbon prepared from tobacco residues: equilibrium, kinetics and thermodynamics. *Journal of Hazardous Materials* **189**, 397–403.

Krishna, K. C. B., Aryal, A. & Jansen, T. 2016 Comparative study of ground water treatment plants sludges to remove phosphorous from wastewater. *Journal of Environmental Management* **180**, 17–23.

Li, Z., Jiang, N., Wu, F. & Zhou, Z. 2013 Experimental investigation of phosphorus adsorption capacity of the waterworks sludges from five cities in China. *Ecological Engineering* **53**, 165–172.

Mortula, M. M. & Gagnon, G. A. 2007 Alum residuals as a low technology for phosphorus removal from aquaculture processing water. *Aquacultural Engineering* **36**, 233–238.

Ng, C., Losso, J. N., Marshall, W. E. & Rao, R. M. 2002 Freundlich adsorption isotherms of agricultural by-product-based powdered activated carbons in a geosmin-water system. *Bioresource Technology* **85**, 131–135.

Razali, M., Zhao, Y. Q. & Bruen, M. 2007 Effectiveness of a drinking-water treatment sludge in removing different phosphorus species from aqueous solution. *Separation and Purification Technology* **55**, 300–306.

R Core Team 2019 *R: A Language and Environment for Statistical Computing*. R Foundation for Statistical Computing, Vienna, Austria. Available from: https://www.R-project.org/ (accessed 21 July 2019).

Yang, Y., Zhao, Y. Q., Babatunde, A. O., Wang, L., Ren, Y. X. & Han, Y. 2006 Characteristics and mechanisms of phosphate adsorption on dewatered alum sludge. *Separation and Purification Technology* **51**, 193–200.

First received 10 July 2020; accepted in revised form 3 November 2020. Available online 13 November 2020